Natural radioactivity of a copper-zinc mine with a production facility in Türkiye and radiological consequences of the usage of tailing as a concrete additive

Aydın Parmaksız*[1], Yücel Özer Özkök[1], Yusuf Ağuş[1]

[1] *Turkish Energy, Nuclear and Mineral Research Agency, Nuclear Energy Research Institute, Atom Street, No:27, 06980, Kahramankazan, Ankara, Türkiye.*

[*]Corresponding author: Aydin.Parmaksiz@tenmak.gov.tr

Abstract

The dose rates of an underground copper-zinc mine and the radioactivities of collected samples were measured using a surveymeter and a gamma-ray spectrometer. There was no significant difference found between mine dose rates and background radiation in the region. The average activity concentrations of ^{226}Ra, ^{232}Th, and ^{40}K in tailing samples were found to be 27%, 83%, and 71% higher than in ores, respectively. It was determined that a miner who worked in the mine for a year and was exposed to the natural radiation of the mine could be exposed to a radiation dose of less than 1 mSv. The annual radiation dose of a person living in a standard concrete room with a certain amount of tailing added to the concrete content was calculated to be 202.2 μSvy^{-1}. Using tailings as concrete additives can help reduce waste released into the environment and make better use of natural resources.

***Keywords**: Copper, Tailing, Dose Rate, Activity Concentration, Radiation Dose, RESRAD-BUILD.*

Introduction

Natural radionuclides are found in all substances in the earth's crust. Radionuclides in the natural radioactive series have had a tendency to decay into stable isotopes via radioactive decay since the beginning of time. These radionuclides are found in low concentrations in most areas, but they can be found in high concentrations in specific areas depending on geological structure. Therefore, radioactivity detection and radiological evaluation of these materials are critical in terms of radiation safety for both the general public and workers.

Ores used in metal production are one of the substances that can be found in high concentrations in nature. In ore deposits, parents and daughters of nuclei from the uranium and thorium series, as well as ^{40}K, can be found in high concentrations. Concentrations of these radionuclides can also rise to dangerous levels following the extraction and processing of mineral ores [1–13]. Radionuclides condense, especially in waste, and can accumulate to levels that are hazardous to the environment and human health.

Because of its strong electrical and thermal conductivities, corrosion resistance, and ductile qualities, copper has become the world's second-most-used metal, with consumption now exceeding thirteen million metric tonnes [14]. According to World Mining Records 2019, global copper production has surpassed 20 million metric tonnes [15]. Despite its high demand and use, copper mining and processing are not so innocent in term of environmental and radiological consequences [16]. Flotation wastes account for 96 percent of the ore mass generated globally, according to 2011 statistics [17]. As a result of copper extraction during manufacturing, highly hazardous metals such as Cd, Fe, Pb, Zn, and As are found in waste [18]. Furthermore, natural radionuclides in ores condense and transfer into flotation wastes as a result of physical and chemical processes during separation. Generally, these wastes are discharged into the seas and oceans via the deep discharge method.

Copper ore can be found in many different minerals. Because of its geochemical properties, copper ore is also related to gold, silver, and uranium [1]. In a scientific study, the highest ^{226}Ra, ^{228}Th, and ^{238}U activity concentrations in water samples were found to be 4.81 BqL^{-1}, 4.51 BqL^{-1}, and 25 BqL^{-1}, respectively [19]. An investigation of an iron-oxide-copper-gold ore deposit found that the maximum activity concentrations of ^{226}Ra, ^{232}Th, and ^{40}K in solid samples were 1699 Bqkg^{-1}, 92.7 Bqkg^{-1}, and 1345 Bqkg^{-1}, respectively [20]. Another study reported ^{238}U activity ranging from 13.8 Bqkg^{-1} to 203.9 Bqkg^{-1} in molybdenum, copper, and gold-polymetallic ore mines [21]. It is known that the concentration of ^{226}Ra in copper ore and waste reached 7216 Bqkg^{-1} and in water, up to 160 Bqkg^{-1} [1, 22]. Since copper ore is usually mined underground, it's important to know how much radioactivity is in the ore, the products, and the waste. It's also important to make radiological assessments based on these contents to make sure that both underground miners and people who work in production are safe from radiation.

Industrial waste, like copper tailings, that can't be recycled and can't be used at all can cause a lot of damage to the environment when they are dumped into the sea or ocean [23–28]. However, by immobilising industrial waste and reusing it in appropriate industries, it is possible to reduce the harmful effects on the environment while also helping to protect natural resources and sustainably develop. Copper tailings can be used as additives in concrete just as waste fly ash from thermal power plants is used as a cement additive. There are also studies in the literature that show that using copper tailings as an additive in concrete at certain rates has both positive environmental effects and improves concrete performance in a variety of ways [29-31]. When copper tailings are added to concrete, its workability, long-term strength, and durability are clearly improved; the homogeneity, microstructure, and pore structure of the concrete improve; and the corrosion start of the concrete is delayed.

Çayeli copper mine and production facilities are located within the borders of Madenli Town, Turkiye, approximately 7 kilometres from Çayeli Town on the Black Sea coast of Turkiye. For more than 20 years, the Çayeli copper mine and production plant has been producing underground copper and zinc concentrates that are marketed and delivered not only to the domestic market but also to the rest of the world [32]. The Çayeli mine and processing complex has an annual ore production and processing capacity of 1.1 million metric tonnes, and it produces one-third of the country's copper [32]. Although the Çayeli mining and production facility has piqued the interest of many academics due to its current potential, no research has been conducted on the complex from a radiological standpoint [16, 33, 34].

In this study, natural radioactivity dose rate measurements were taken with a surveymeter in the areas where workers in the Çayeli underground mining areas work. Samples were taken from the ores, some materials in the production stages, end products, and wastes at the mine site. In accredited laboratories, gamma spectrometric analyses of the samples were done, and radiological evaluation indices were calculated. Simulation software was used to test whether flotation wastes could be used in concrete from a radiological point of view, and based on the results, radiological evaluations were done.

Materials and Methods

Dose rate measurements

At the Çayeli mine, which is operated as recyclable and backfilled within the framework of the room-and-pillar mining process, the ore is brought to the surface by elevator. The vacated area is filled with crushed stone, sand, and cement. While the mining activities were carried out continuously due to the new excavations in the mine, within the scope of the study, dose rate measurements were taken from various points in the mine, from 80 metres above sea level (the main transport well) to 430 metres below sea level (the 570 shaft).

The dose rate measurements due to natural radioactivity inside the mine were performed at the selected points using the Radiagem^{TM}2000 personal portable survey meter with an energy-compensated GM detector at a height of 1 m above ground. A personal portable survey meter has dimensions of 150 x 85 x 45 mm and is capable of measuring gamma and x-ray photons in the energy range of 40 keV to 1.5 MeV. It has a measurement range of 0.01 μSvh^{-1} to 100 $mSvh^{-1}$ and an external, 3.3-meter wide-range telescopic probe. The Radiagem^{TM}2000 personal portable survey meter has a sensitivity of 0.83 c/s per µSv/h. The accuracy given by the manufacturer is ±15%.

The Turkish Energy, Nuclear, and Mineral Research Agency's (TENMAK) Nuclear Energy Research Institute (NÜKEN) has secondary standard dosimetry laboratories. The services provided by the Secondary Standard Dosimetry Laboratory (SSDL) in the NÜKEN Ankara Campus have been accredited by the Turkish Accreditation Agency (TÜRKAK) to include all measurement quantities within the scope of accreditation according to the TS EN ISO/IEC 17025 standard. It became a full member of the Secondary Standard Dosimetry Laboratories Network (IAEA/WHO SSDL Network), created by the International Atomic Energy Agency (IAEA) and the World Health Organization (WHO), on March 24, 2020. Radiagem™2000 personal portable survey meter are calibrated every two years at the NUKEN Secondary Standard Dosimetry Laboratory.

Gamma Calibration System-Protection Level and ISO 4037 Standard were used for Radiagem™2000's calibration in SSDL. The calibration conditions were 20±2 ºC, 950±50 hPa, and 50±20% for temperature, pressure, and humidity, respectively. The device is calibrated on the ISO Water Slab Phantom. The reference point of the detector is aligned with the radiation beam axis using lasers. The last line in the table corresponds to a measurement carried out in the dose register mode of the device. The error margin is accepted to be ±15% for dose rate meters. A ^{137}Cs radionuclide was used for calibration. Dose rates were used between $5.0x10^{-6}$ Svh^{-1} and $2.5x10^{-2}$ Svh^{-1} for calibration. Total uncertainties were found to be between 11.0 and 6.1%. The expanded uncertainty of measurement is stated as the standard uncertainty of the measurement multiplied by the coverage factor k = 2, which for a normal distribution corresponds to a coverage probability of approximately 95%.

Sampling and sample preparation

Galena (PbS), sphalerite (ZnS), chalcopyrite ($CuFeS_2$), bornite (Cu_5FeS_4), and pyrite (FeS_2) are the primary minerals discovered at the Çayeli mine [35]. Based on its physical structure, Çayeli ore is classified into three types: zinc-rich black ore; copper-rich yellow ore; and clastic ore, which contains both copper and zinc as well as quartz and barite. If the sphalerite ratio in the mined ore is less than 10%, the ore is called yellow ore, and if it is more than 10%, it is called black ore.

After the ore production operations in the mine, production starts from the stockpiles to the final product and waste. Following underground production, the ores are transported to the surface by elevator and delivered to one of the eight parts of the stockpile, which are divided into eight sections based on the mineral concentration of the ores. After being treated by an enrichment process, the impurities in the ore are separated and formed into clusters. The copper concentrate is an ore whose copper concentration has increased significantly as a consequence of this procedure. It is crushed to a suitable fineness and ground in the first step of enrichment to remove the undesirable minerals in the ore. The copper and zinc concentrates are then precipitated in the flotation cycle, and the finished product is produced in the filters. The waste created during the process is then discharged into the sea by pipes that are 3 kilometres off shore and 380 metres deep [35].

To begin with, the locations to be worked in the facility's production processes were selected, and a total of twenty-eight samples were gathered, with eleven being ore, six being copper, three being zinc, and eight being tails. Seven ore samples were taken from the stockpile: two from the secondary ball mill, one from the crasher, and one from the fine ore bin. Four of the copper samples were taken from the rougher and two from the final copper product. One zinc sample came from the rougher, while the other two came from the finished zinc products. Four tailings samples were obtained from the rougher, two from the cleaner, and two from the final waste during the process.

The samples collected on the job site were placed in 1- to 1.5-liter plastic bags, labelled, and the mouths of the bags were tightly tied. The samples were packed in such a way that they would not be harmed during transportation and brought to TENMAK-NÜKEN [36]. The samples were prepared for examination in the Gamma Spectrometry Laboratory's sample preparation unit in the Radioactivity and Analytical Measurement department using standard sample preparation techniques.

Using a sieve, undesired particles such as plant parts, stones, and other contaminants were removed from samples and delivered to the laboratory. To minimise particle sizes, solid materials in rock form were ground in a mill. To eliminate moisture from the samples, they were maintained at 105 °C for ten hours in a temperature-controlled drying oven. After cooling, the samples taken from the oven were placed in cylindrical plastic analysis containers with a diameter of 6 cm and a height of 5 cm and weighed. The samples were hermetically wrapped with parafilm and left for 30 days before analysis to bring the ^{226}Ra into secular equilibrium with the short-half-life daughters ^{214}Pb and ^{214}Bi, since the activity concentration of ^{226}Ra was calculated from its product nuclei.

According to the validation report, the largest contribution to the combined uncertainty budget used in radioactivity measurements comes from the homogeneity of the sample preparation processes. Uncertainty due to contamination or loss of the sample, uncertainty in the sample mass or volume, uncertainty due to sample homogeneity, and uncertainty due to the preconcentration procedure are the sources of uncertainties regarding the sample preparation. For the homogeneity test, 20 samples have been prepared. Two groups of ten from each of the samples are randomly selected, and two new groups are created. All samples in these two new groups are randomly chosen and measured. An ANOVA test has been applied to the measurement results to calculate the degree of homogeneity. Calculated sample preparation uncertainty values have been inserted into the combined uncertainty in the validation report [37].

Radioactivity Measurements

The Nuclear Energy Research Institute, which is succeeding the Turkish Atomic Energy Agency (TAEA), is one of five institutions of the Turkish Energy, Nuclear, and Mineral Research Agency (TENMAK) and has two campuses in Ankara and Istanbul [36]. These analyses were performed at NÜKEN's Gamma Spectrometry Laboratory (GML), which has been accredited by the Turkish Accreditation Agency (TURKAK) in Ankara. GML was accredited in 2009, and it has been participating in international comparison tests and being audited annually by TURKAK auditors since then, in compliance with accreditation regulations.

GML now operates ten gamma-ray measurement systems outfitted with Ortec and Canberra brand high purity germanium detectors (HPGe) with liquid nitrogen cooling. The HPGe detector's relative efficiencies range from 10 to 150 percent, and data analysis software such as Gammavision-32 and Genie-2000 was installed on the systems. The gamma-ray spectrometer used in this investigation has the following technical parameters: A Canberra brand p-type HPGe detector and a DSA-1000 multichannel analyzer are used in the gamma-ray spectrometry system. The active volume of HPGe is 451 cm^3. It has an 85:1 peak-to-Compton ratio and a 110 percent relative efficiency. The energy resolutions of the HPGe are 2.1 keV (for the 1332.5 keV energy of ^{60}Co) and 1.3 keV (for the 122 keV energy of ^{57}Co).

The HPGe detector is enclosed in a shield that may be opened from the top and sides to limit the input of natural background radiation. This shielding consists of a 10 cm-thick lead layer, a 1 mm-thick tin layer, a 1.5 mm-thick copper layer, and a 9.5 mm-thick steel outer body.

In a time period short enough for energy calibration, ^{241}Am, ^{137}Cs, and ^{60}Co standard point sources were counted in the gamma-ray spectrometer. To find unknown gamma-ray emitters, a best-fit function of the energy corresponding to each channel in the multichannel analyzer was plotted using the data taken from this spectrum [37]. The absolute efficiency calibration of the HPGe detector was performed by counting volumetric sources with exactly the same geometry, nearly the same density, and the same chemical composition as the sample under study [37]. The reference materials RGU-1 (U ore), RGTh-1 (Th ore), and RGK-1 (K_2SO_4), which are certified radioactive standard volume sources produced by the International Atomic Energy Agency, were measured by placing a counting container (6 cm in diameter and 5 cm in height) that has the same geometry as the sample analysis containers [38]. In this study, the method of comparing the standard with the sample, which is also known as "determining activity concentration by comparing the net count rate of the sample with the net count rate of standard reference material," was used [39]. Because of the overlap of 185.7 keV of ^{235}U, analysis of the samples was done using the gamma ray energies of ^{214}Pb (295.2 keV and 351.9 keV) and ^{214}Bi (609.3 keV) for measurement of the activity concentration of ^{226}Ra instead of its own energy [40]. In this work, the activity concentration of ^{232}Th was determined from the 338.3 keV and 911.2 keV energies of ^{228}Ac, which is the daughter product of ^{232}Th, while the single energy of ^{40}K was found to be 1460.8 keV [40]. The formula for determining sample activity concentrations is given below [41].

$$A = N_p/[\varepsilon(E_\gamma) \times P_\gamma \times M] \qquad (1)$$

Where Np denotes the net count rate of the sample, $\varepsilon(E_\gamma)$ is the efficiency value for interested energy, P_γ is the abundance of the γ-line in a radionuclide, and the last symbol M stands for the mass of the sample as a kilogramme [40]. The formula for computing minimum detectable activity (MDA) levels is as follows [42]:

$$MDA = 1.64\sigma_n/[\varepsilon(E_\gamma) \times P_\gamma \times t \times M] \qquad (2)$$

This formula represents the standard deviation of the background in the region of interest (equal to the square root of the number of counts for the background spectrum) and the measurement duration in seconds by σ_n and t, respectively [40].

Results and Discussion

Results of mine dose rate measurements

Table 1 shows the locations of the gamma dose rate measurement points in the Çayeli underground copper-zinc mine, as well as their height above sea level, coordinates for certain spots, and measurement results. As can be seen in Table 1, the measured dose rates in the mine vary between 0.1 μSvh^{-1} and 0.3 μSvh^{-1}, and their geometric mean is calculated at 0.2 μSvh^{-1}. The Radiation Early Warning System Network (RESA) in Türkiye collects immediate radiation dose rate data from 211 locations [43]. This data is transmitted to EURDEP, the European Radiological Data Exchange Platform, and the data supplied to EURDEP by European nations is checked on a regular basis [44]. The average terrestrial gamma radiation rate observed at the RESA station in Rize Province, where the Çayeli area is located, is approximately 90 $nSvh^{-1}$. Despite the fact that the average gamma dose rate (160 $nSvh^{-1}$) observed in the mine in this work was somewhat greater than the natural background level, no significant difference was found. It is possible to find research with similar, lower, or higher values related to underground mining in the literature [45–50]. The maximum annual radiation dose that a person working in this mine for 1800 hours per year can get has been determined to be 558 μSv (0.6 mSv). This value was found to be less than 1 $mSvy^{-1}$, which is the reference value given to the public [51].

Table 1. Çayeli underground copper-zinc ore mine dose rate measurement results

Location description	Coordinates (WGS 84)		Altitude above sea level	Dose rate (μSvh^{-1})
	Latitude	Longitude		
Main transport well	41° 02’ 23.70’ N	40° 45’ 50.49’ E	+80	0.1
Main transport well			+80	0.1
Main transport well			+80	0.3
Main transport well			+80	0.3
1060 XC (Cross cut)	41° 02’ 20.97’ N	40° 45’ 50.49’ E	+60	0.2
1040 Backfill	41° 02’ 23.70’ N	40° 45’ 46.56’ E	+40	0.1
980 HWS (Hanging wall south)	41° 02’ 23.35’ N	40° 45’ 48.04’ E	-20	0.1
960 HWS (Hanging wall south)	41° 02’ 21.53’ N	40° 45’ 46.02’ E	-40	0.1
940 Refectory			-60	0.2
840 FWN (Foot wall north)	41° 02’ 28.35’ N	40° 45’ 52.07’ E	-160	0.2
800 Mechanic (Underground Mechanical workshop)	41° 02’ 24.36’ N	40° 45’ 58.09’ E	-180	0.1
800 N 15 (North)	41° 02’ 27.41’ N	40° 45’ 51.87’ E	-200	0.2
790 XCS (Cross cut south)	41° 02’ 20.87’ N	40° 45’ 47.24’ E	-210	0.1
775 Lubrication station	41° 02’ 27.08’ N	40° 45’ 52.16’ E	-225	0.2
685 Refectory	41° 02’ 23.63’ N	40° 45’ 53.57’ E	-315	0.3
620 Ore pass			-360	0.2
650 Ore pass			-390	0.1
570 Shaft	41° 02’ 23.02’ N	40° 45’ 52.95’ E	-430	0.2

Radioactivity measurement results

Table 2 shows the findings of the gamma spectrometric analyses of the samples used in this work. The highest, lowest, and mean values of ^{226}Ra activity concentrations in copper ore samples were determined to be 155±24 $Bqkg^{-1}$, 14±2 $Bqkg^{-1}$, and 64 $Bqkg^{-1}$, respectively. The activity concentrations of ^{232}Th ranged from MDA to 10±2 $Bqkg^{-1}$, with an average of 4 $Bqkg^{-1}$. The average ^{40}K activity concentration was 55 $Bqkg^{-1}$, ranging from the MDA value to 120±22 $Bqkg^{-1}$. The average activity concentrations of ^{226}Ra, ^{232}Th, and ^{40}K in crustal earth soil were reported by UNSCEAR to be 32 $Bqkg^{-1}$, 45 $Bqkg^{-1}$, and 412 $Bqkg^{-1}$, respectively [52]. The activity concentrations of ^{232}Th and ^{40}K were found to be much lower than the earth's crust averages. Despite the fact that the ^{226}Ra activity concentration is somewhat greater than the average of the earth's crust, the levels detected might be considered modest for ores.

The average ^{226}Ra activity concentration was determined to be 55 $Bqkg^{-1}$ in analyses of six copper concentrate samples obtained from various locations of the plant, with the highest result being 89±15 Bqkg^{-1}. The majority of the ^{232}Th and ^{40}K activity concentrations were lower than the MDA levels; only ^{232}Th in two samples and ^{40}K in three samples were detected at low levels. The average ^{226}Ra activity concentration was found to be 83 Bqkg^{-1} in three zinc samples, whereas ^{232}Th activity concentrations were found to be relatively low, or below the MDA value. The explanation for the higher than usual ^{226}Ra activity concentration in the zinc sample collected from the rougher feed is that the separation process has not yet been finished, so the feed still contains a significant quantity of ore.

Table 2. Gamma spectrometric analysis results of the samples

Sample No	Sample/ sampling location	^{226}Ra (Bqkg^{-1})	^{232}Th (Bqkg^{-1})	^{40}K (Bqkg^{-1})
1.	Clastic Ore (stockpile)	74±13	<1	<10
2.	Clastic Ore (stockpile)	35±7	2±1	10±3
3.	Clastic Ore with bornite (stockpile)	57±3	<1	84±9
4.	Black Ore-a (stockpile)	98±17	<1	<20
5.	Black Ore-b (stockpile)	100±18	4±1	13±4
6.	Yellow Ore (stockpile)	29±3	<2	54±4
7.	Low Grade Ore (stockpile)	87±14	10±2	120±22
8.	Ore (crasher)	36±7	3±1	55±9
9.	Ore (fine ore bin)	23±8	5±2	23±8
10.	Ore (secondary ball mill)	14±2	<1	<10
11.	Ore (secondary ball mill)	155±24	10±2	85±17
12.	Copper Rougher Concentrate-a	38±8	<4	<20
13.	Copper Rougher Concentrate-b	41±2	<6	<20
14.	Copper Rougher Tail-a	83±12	7±1	113±16
15.	Copper Rougher Tail-b	78±3	8±2	113±7
16.	Copper Rougher Scavenger Concentrate	57±8	<1	<10
17.	Copper Rougher Columns Concentrate	51±6	6±1	29±4
18.	Copper Rougher Columns Tail	102±15	6±1	99±15
19.	Copper Cleaner Tail (Combined)-a	9±1	<1	8±1
20.	Copper Cleaner Tail (Combined)-b	118±12	8±2	<17
21.	Copper Rougher Scavenger Tail	60±7	<5	<20
22.	Zinc Rougher Feed	148±12	8±1	75±15
23.	Final Tail-a	108±8	10±1	107±8
24.	Final Tail-b	95±5	9±1	127±13
25.	Copper Final Concentrate-a	89±15	<1	10±3
26.	Copper Final Concentrate-b	57±7	45±1	23±4
27.	Zinc Final Concentrate-a	61±11	<1	10±5
28.	Zinc Final Concentrate-b	41±5	3±1	<10
	Mean ± SD	69±38	9±10	61±44

The value to the right of the "<" symbol shows the minimum detectable activity (MDA).

Tailing is an unintended byproduct of the physical and chemical operations of mining facilities. Because it contains hazardous compounds as well as radionuclides, it is not easily recyclable and is discharged directly into the sea. In this investigation, the activity concentrations of ^{226}Ra radionuclide in eight tailing samples ranged from 8.8±1.3 $Bqkg^{-1}$ to 118±12 $Bqkg^{-1}$, with an average of 82±35 $Bqkg^{-1}$. In the aforementioned samples, the average activity concentrations of ^{232}Th and ^{40}K radionuclides were determined to be 7±3 $Bqkg^{-1}$ and 94±43 $Bqkg^{-1}$, respectively. The IAEA recommended that radionuclides of natural origin be excluded from regulatory control at the following levels: 1 Bqg^{-1} for ^{226}Ra and ^{232}Th radionuclides and 10 Bqg^{-1} for ^{40}K radionuclides [53]. All the measured activity concentrations given in Table 2 were determined to be below the IAEA's suggested regulatory control threshold.

Figures 1, 2, and 3 show the frequencies of activity concentrations of ^{226}Ra, ^{232}Th, and ^{40}K radionuclides in samples, respectively. The maximum number of samples was determined to be between 40 $Bqkg^{-1}$ and 60 $Bqkg^{-1}$ for ^{226}Ra activity concentrations, while no sample was found to be between the 120-140 $Bqkg^{-1}$ range, as seen in Figures 3, 4, and 5. For ^{232}Th activity concentrations, this range was found to be from 6 $Bqkg^{-1}$ to 8 $Bqkg^{-1}$. The maximum number of samples was determined to be between 0 $Bqkg^{-1}$ and 20 $Bqkg^{-1}$ for ^{40}K activity concentrations.

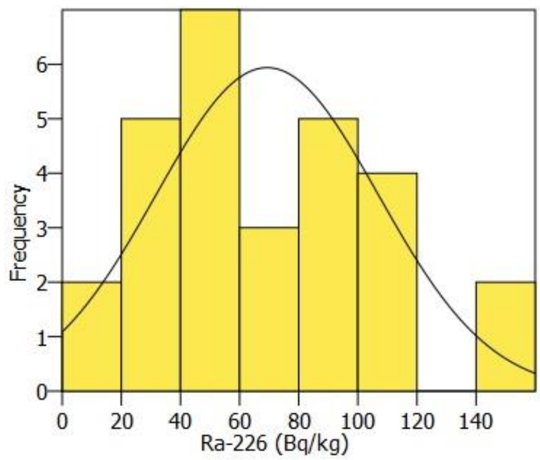

Figure 1. ^{226}Ra radionuclide frequency in samples

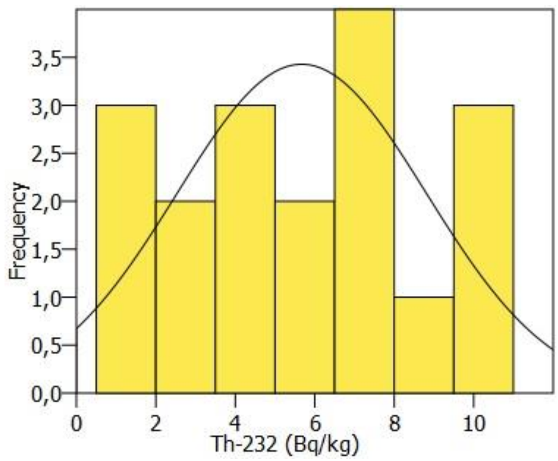

Figure 2. ^{232}Th radionuclide frequency in samples

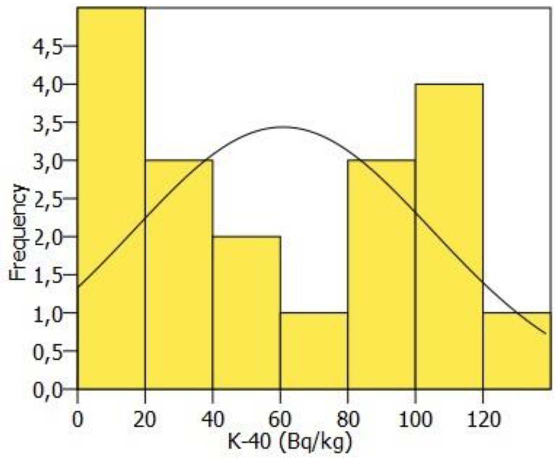

Figure 3. ^{40}K radionuclide frequency in samples

Increased concentrations of natural radionuclides in products or waste materials as a result of industrial human operations such as manufacturing, mineral extraction, or water processing are referred to as “technologically enhanced NORM (naturally occurring radioactive material)" or "TENORM (technologically enhanced naturally occurring radioactive material)” [1]. Because the average activity concentrations of ^{226}Ra, ^{232}Th, and ^{40}K in tailing samples were found to be 27%, 87%, and 71% higher than the aforementioned average radionuclide concentrations in ores, respectively, tailing samples may be classified as TENORM, and the copper industry may also be accepted as a TENORM producer. Therefore, the radiological assessment of the tailing samples accepted as TENORM was done using the radiological indices calculated below, and the findings are shown in Table 3.

Table 3. Radiological evaluation indices of tailing samples

Sample No	Sample	Ra_{eq} ($Bqkg^{-1}$)	I_{γ}	I_{α}	D ($nGyh^{-1}$)	E ($mSvy^{-1}$)	ELCR
1	Copper Rougher Tail-a	101±12	0.3	0.4	93	0.5	$1{,}9x10^{-3}$
2	Copper Rougher Tail-b	98±4	0.3	0.4	89	0.4	$1{,}8x10^{-3}$
3	Copper Rougher Columns Tail	118±15	0.4	0.5	108	0.5	$2{,}2x10^{-3}$
4	Copper Cleaner Tail (Combined)-a	10±1	0.0	0.0	10	0.1	$1{,}9x10^{-4}$
5	Copper Cleaner Tail (Combined)-b	129±12	0.4	0.6	117	0.6	$2{,}4x10^{-3}$
6	Copper Rougher Scavenger Tail	60±7	0.2	0.3	55	0.3	$1{,}1x10^{-3}$
7	Final Tail-a	131±8	0.4	0.5	119	0.6	$2{,}4x10^{-3}$
8	Final Tail-b	118±5	0.4	0.5	107	0.5	$2{,}2x10^{-3}$

Radiological indices of tailing samples

Many indices have been created to help in the radiological evaluation of radioactive wastes. The “Radium Equivalent Activity (Ra_{eq})” formula, which was designed for the assessment of materials having ^{226}Ra, ^{232}Th, and ^{40}K activity concentrations and is one of the most extensively used indices in the literature, is provided below [54, 55]:

$$Ra_{eq} = A_{Ra} + 1.43A_{Th} + 0.077A_K \qquad (3)$$

where A_{Ra}, A_{Th}, and A_K indicate the activity concentrations of ^{226}Ra, ^{232}Th, and ^{40}K in $Bqkg^{-1}$, respectively. Samples with radium equivalent activities less than 370 $Bqkg^{-1}$ are accepted for use in building materials. The highest Ra_{eq} value found in the tailing samples studied was 131±9

$Bqkg^{-1}$. Because all tailing samples are less than the 370 $Bqkg^{-1}$ limit value, it is possible to declare that tailing samples can be used safely in construction materials.

The activity concentration index (I_γ) is calculated to determine if the annual radiation dose due to excess external gamma radiation in a building is greater than 1 mSv [56]. If the unitless activity concentration index is greater than one, the annual radiation dose from the building materials under consideration is also greater than 1 mSv. An activity concentration index of less than 0.5 indicates that the annual radiation dose for bulk materials such as concrete is less than 0.3 mSv; less than 1 indicates that the annual radiation dose is less than 1 mSv. With an activity concentration index of less than 2, the annual radiation dose from surfaces and other restricted-use materials (tiles, boards, etc.) is less than 0.3 mSv, and with an index of less than 6, the annual radiation dose is less than 1 mSv. The formula for calculating the activity concentration index is presented below [56].

$$I_\gamma = \frac{A_{Ra}}{300\ Bqkg^{-1}} + \frac{A_{Th}}{200\ Bqkg^{-1}} + \frac{A_K}{3000\ Bqkg^{-1}} \qquad (4)$$

A_{Ra}, A_{Th}, and A_K represent the ^{226}Ra, ^{232}Th, and ^{40}K activity concentrations in the $Bqkg^{-1}$ unit in the building materials. The highest value of the activity concentration indexes of eight tailing samples was 0.4, while their mean value was 0.3. These findings indicate that using tailing samples from the Çayeli plant is radiologically safe for both bulk materials like concrete and surfaces and other restricted-use materials in building materials.

The alpha index (I), another radiological assessment measure, was developed to evaluate the inhaled alpha radiation from ^{222}Rn that had leached from construction materials using the following formula [57]:

$$I_\alpha = \frac{A_{Ra}}{200\ Bqkg^{-1}} \qquad (5)$$

A_{Ra} represents the activity concentration of the building materials in the $Bqkg^{-1}$ unit. If the I_α value is less than or equal to one, the ^{222}Rn activity concentration in building materials is regarded as being less than or equal to the acceptable indoor ^{222}Rn activity concentration of 200 Bqm^{-3}. The alpha indices of eight tailing samples had a maximum value of 0.6 and a mean value of 0.4. Based on the fact that all I_α values were found to be less than one, it can be concluded that if tailing samples are used to build the standard room, the ^{222}Rn activity concentrations will remain below the recommended threshold of 200 Bqm^{-3}.

The indoor gamma dose rate (D_R) due to gamma rays emitted from ^{226}Ra, ^{232}Th, and ^{40}K radionuclides in building materials in a standard room was calculated using the formula given below [56, 57].

$$D_R = 0.92A_{Ra} + 1.10A_{Th} + 0.08A_K \qquad (6)$$

The acronyms A_{Ra}, A_{Th}, A_K, and D_R refer to the activity concentrations in $Bqkg^{-1}$ units of ^{226}Ra, ^{232}Th, and ^{40}K radionuclides in building materials, as well as the indoor gamma dose rate in $nGyh^{-1}$ units, respectively. In this study, the indoor gamma dose rate of eight tailing samples varied from 9 $nGyh^{-1}$ to 119 $nGyh^{-1}$, with an average of 87 $nGyh^{-1}$. The maximum global indoor gamma-absorbed dose rate was reported as 200 $nSvh^{-1}$, while the population-weighted average of it was given as 84 $nSvh^{-1}$ [58]. This study's maximum global indoor gamma absorbed dose rate is lower than reported values and quite close to the population-weighted average indoor gamma absorbed dose rate [58].

The following formula was used to calculate the annual effective dose in $mSvy^{-1}$ units, which corresponds to the indoor gamma dose rate [58]:

$$E_R = D_R \times C_F \times OF \times T \times 10^{-6} \qquad (7)$$

where D_R, C_F, OF, and T denote the indoor absorbed gamma dose rate; the dose conversion factor, which has a value of 0.7 $SvGy^{-1}$; the occupancy factor, which has a value of 0.8; and the duration, which has a value of 8766 hy^{-1}. The maximum annual radiation dose to which a member of the public can be exposed in a standard concrete room constructed with tailing samples was calculated to be 0.6 mSv. The average indoor effective dose value derived from tailing samples was found to be the same as the global average indoor effective dose of 0.4 $mSvy^{-1}$ [58]. The computed maximum annual effective dose value was determined to be less than 1 $mSvy^{-1}$, which is the public's recommended reference level for radiation exposure from building materials [59].

The following equation was used to calculate excess lifetime cancer risk (ELCR) based on calculated annual effective dose values [60]:

$$ELCR = E_R \times LE \times RF \qquad (8)$$

where E_R is the indoor annual effective dose calculated by equation 7, LE is the life expectancy of 73 years given in the latest world average data by the World Health Organization (WHO), and FR is the fatal risk factor of 5.7×10^{-2} Sv^{-1} given by the ICRP in 1990 [61, 62]. In this investigation, the lowest and highest ELCR values originated from eight tailing samples were determined to be 1.9×10^{-4} and 2.4×10^{-3}, respectively, with a mean value of 1.8×10^{-3}. This study's ELCR value of 1.8×10^{-3} is also highly consistent with the 1.7×10^{-3} value estimated based on the global average indoor effective dose value of 0.4 $mSvy^{-1}$ and the latest average life expectancy of 73 years.

The effective dose for a person living in a concrete room with added copper tailings

Many plants dispose of copper tailings as non-recyclable waste, but copper tailings are actually recyclable waste [63–69]. It was stated in literature that using copper tailings as an additive in concrete improves its performance in a variety of ways and has a favourable impact on the environment. Research found in the literature shows that copper tailings are added to concrete at different rates, ranging from 5% to 30%, depending on the properties being studied. Adding more than 30% of copper tailings is not recommended for a number of reasons [70]. However, in order to evaluate potential radiological health impacts, the increased radiation dose of a member of the public living in a concrete room with a copper tailing addition must be computed. Consequently, the additional radiation doses from copper tailing for a person spending an entire year in a standard concrete room containing 30% copper tailing were calculated using the RESRAD-BUILD simulation software developed by Argonne National Laboratory [71]. The RESRAD-BUILD software can calculate external radiation doses from radioactive sources, inhalation doses from dust and radon gas, and ingestion doses from unintentional swallowing of suspended radioactive particles in air.

In this study, standard model room parameters from the European Commission Office's European Commission Report on Radiological Protection Principles Concerning the Natural Radioactivity of Building Materials were utilised for the computations [56]. The model room described in the RP 112 report has dimensions of 4 m x 5 m x 2.8 m, and its floor, ceiling, and walls have a density of 2.35 gcm^{-3} and a thickness of 20 cm. The calculations assumed that 30 percent tailing was added to the walls, floor, and ceiling of the room and that the radiation sources were rectangular volumetric radiation sources. The receiver is assumed to be standing at the intersection of the room's floor diagonals for 7000 h, and calculations are based on a one-metre height from the floor (Figure 4).

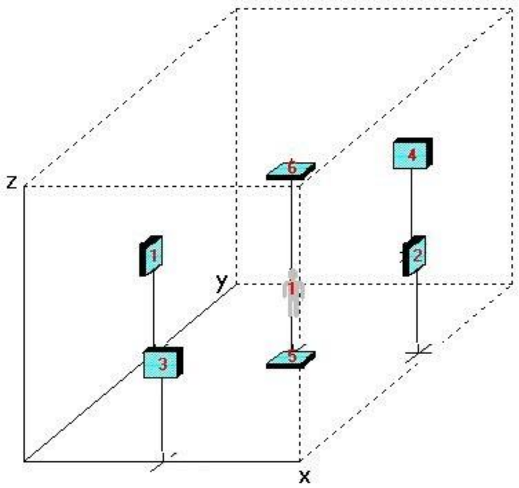

Figure 4. Receptor and sources in the model room

In the calculations, the mean tailing activity concentrations for each radionuclide and the most reasonable parameters from the scientific literature were utilised [40, 72–75]. The simulation parameters for the exposure scenario performed in this study are shown in Table 4.

Table 4. RESRAD-BUILD simulation parameters [40].

Simulation Parameters	Values
Room dimensions	4 m x 5 m x 2.8 m
Thickness of floor, ceiling and wall	20 cm, 20 cm, 20 cm
Density of concrete	2.35 g cm^{-3}
Total surface area of model room	90.4 m^2
Volume of model room	56 m^3
Indoor/time fraction	0.8
Number of room/occupants	1/1
Deposition velocity	1×10^{-2} m s^{-1}
Resuspension rate	5×10^{-7} s^{-1}
Breathing rate	18 m^3 d^{-1}
Ingestion rate	0 g h^{-1}
Occupant location in the room	1 m above on the floor and centred
Shielding thickness	0 (no shielding)
Type of source	Volume (x-, y and z-direction)
Source geometry	Rectangular
Release air fraction	0.1
^{222}Rn diffusion rate	2×10^{-5} m s^{-1}
Erosion rate	2.4×10^{-8} cm d^{-1}
Building air exchange rate	8×10^{-1} 1 h^{-1}

The annual additional radiation doses that a receptor staying in the model room with a tailing sample added to the concrete of the floor, ceiling, and walls could be exposed to due to this tailing were calculated in this study using the RESRAD-BUILD code parameters (breathing rate, ingestion rate, deposition velocity, resuspension rate, and so on) listed in Table 4. Figure 5 shows the doses of receptors from external, deposition, immersion, inhalation, radon, and ingestion that were calculated for each source using the RESRAD-BUILD computer program.

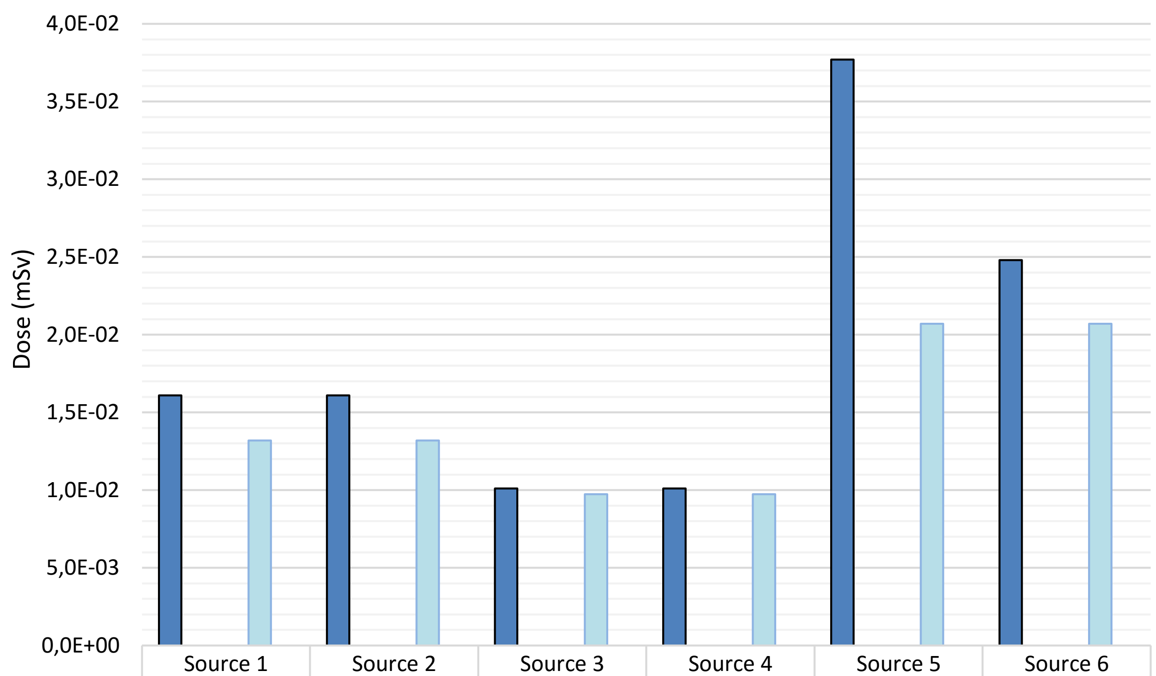

	Source 1	Source 2	Source 3	Source 4	Source 5	Source 6
External	1,6E-02	1,6E-02	1,0E-02	1,0E-02	3,8E-02	2,5E-02
Deposition	4,1E-09	4,1E-09	3,0E-09	3,0E-09	6,4E-09	6,4E-09
Immersion	3,0E-11	3,0E-11	2,2E-11	2,2E-11	4,7E-11	4,7E-11
Inhalation	1,2E-06	1,2E-06	8,8E-07	8,8E-07	1,9E-06	1,9E-06
Radon	1,3E-02	1,3E-02	9,7E-03	9,7E-03	2,1E-02	2,1E-02
Ingestion	5,4E-08	5,4E-08	4,0E-08	4,0E-08	8,5E-08	8,5E-08

Figure 5. Contributions of pathways and sources to the total dose

External radiation, as shown in Figure 5, contributes the most to the radiation dose to which the receptor is exposed. The external radiation dose ranged from 10 μSvy^{-1} to 38 μSvy^{-1}, with an average of 19 μSvy^{-1}. The radon dose from inhaling ^{222}Rn, the decay product of ^{226}Ra, which contributes to the annual dose in a secondary way, was calculated to be between 10 μSvy^{-1} and 21 μSvy^{-1}, with an average of 15 μSvy^{-1}. The deposition, immersion, inhalation, and ingestion doses given in Figure 5 were actually found to be negligibly low when compared to the external and radon doses.

The total annual dose to which the receptor can be exposed via all pathways has been calculated to be 202 μSvy^{-1}. The largest contribution to the total dose comes from source 5 (the floor of the room) with 29%, and the second largest contribution comes from source 6 (the ceiling of the room) with 23%. This means that the floor and ceiling of the room account for more than half of the total contribution. The radiation doses calculated by the RESRAD-BUILD software in this study were found to be less than the annual reference level of 1 mSv set by Council Directive 2013/59 [76].

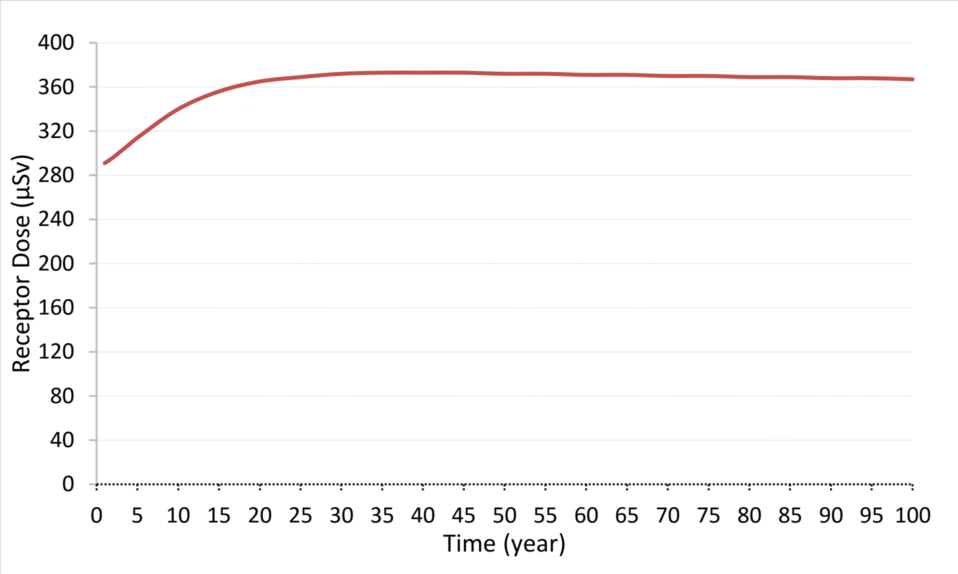

Figure 8. Receptor dose-year averaged over exposure duration relationship

Figure 6 is a graph illustrating the variation of the total dose that a receptor in a room with 30 percent tailing can be exposed to from all paths over a hundred years, as calculated by the RESRAD-BUILD code. The graph shows that the receptor dose increases rapidly in the first six years, and although the rate of increase slows until the thirtieth year, the receptor dose continues to rise. While only ^{226}Ra, ^{232}Th, and ^{40}K radionuclides were present at the start of the simulation, it can be seen that these radionuclides turn into decay products, even slightly, and the radiation dose increases due to the contributions of these decay product radionuclides. ^{228}Th, ^{228}Ra, and ^{210}Pb activity concentrations, which are decay products of ^{232}Th and ^{226}Ra, increase over time. It is seen that it reaches a peak in the thirty-third year, stays there until the thirty-seventh year, and then begins to fall with a slight decrease in activity concentrations.

Conclusions

It is possible to encounter large volumes of waste containing long-lived natural radionuclides in many industries. Due to special processes during production, these radionuclides can exceed natural levels, especially in waste. The public and workers are more likely to be exposed to radiation from this increased natural radionuclide-containing waste and products than from most other sources of radiation. For this reason, it is necessary to reduce the amount of all kinds of waste produced in these sectors and to manage all waste in a way that protects human health and the environment.

In this study, dose rate measurements were made in the underground copper-zinc mine in areas determined to be up to 430 metres below sea level. There was no significant difference found between the average gamma dose rates observed in the mine and the natural background radiation of the region. It was determined that the maximum additional radiation dose (0.6 mSv) that a worker working 1800 hours a year in the mine can be exposed to is less than 1 mSvy^{-1}, which is the reference value for a member of the public.

The maximum sample number in the frequency analysis was determined to be in the range of 40-60 Bqkg^{-1} for ^{226}Ra, 6-8 Bqkg^{-1} for ^{232}Th, and 0-20 Bqkg^{-1} for ^{40}K. All of the samples' activity concentrations were found to be below the recommended levels for radionuclides of natural origin to be exempt from regulatory control. This work determined that tailing wastes may be classified as TENORM since the average activity concentrations of ^{226}Ra, ^{232}Th, and ^{40}K in the tailing samples were, respectively, 27 percent, 87 percent, and 71 percent higher than the corresponding average radionuclide concentrations in the ores.

According to the calculated results of radiological indexes, because all tailing samples have Radium Equivalent Activity Index values of less than 370 $Bqkg^{-1}$, it is possible to state that tailing samples can be safely used in construction materials. The activity concentration indexes of eight tailing samples had a maximum value of 0.4 and a mean value of 0.3. According to these results, using tailing samples from the Çayeli plant is radiologically safe for use in both bulk materials like concrete and surfaces and other restricted-use materials. Because all Alpha indices are less than 1, it is assumed that ^{222}Rn activity concentrations coming from tailing samples will remain below the suggested level of 200 Bqm^{-3} if tailing samples are used to build the standard room.

The maximum global indoor gamma absorbed dose rate in this study is lower than previously published values and relatively close to the population-weighted average indoor gamma absorbed dose rate. The ELCR value of $1.8x10^{-3}$ in this study is likewise comparable to the $1.7x10^{-3}$ value determined based on the global average indoor effective dose value of 0.4 $mSvy^{-1}$ and the most recent average life expectancy of 73 years.

In this study, radiation doses were calculated using the RESRAD-BUILD software for an individual who spent a full year in a conventional concrete room with 30% copper tailing added. The total annual dose to which the receptor can be exposed from all pathways was determined to be 202.2 μSvy^{-1}. The dose from the room's floor and ceiling accounts for more than half of the total dose to which the receptor is exposed. The radiation doses calculated by the RESRAD-BUILD software in this study were found to be less than the annual reference level of 1 mSv.

The tailing, which is a waste product of the copper-zinc production process, is released into nature as an important contaminant without being recycled. Tailing samples, on the other hand, have been shown in studies encountered in the scientific literature to actually be recyclable waste. According to the study's findings, using tailing samples as concrete additives in specific amounts has no negative radiological consequences and can even aid in the efficient use of limited natural resources, resulting in a significant reduction in the amount of pollutants discharged into the environment.

Funding

This study was funded by the Turkish Energy, Nuclear, and Mineral Research Agency and carried out as part of the research activities of the Nuclear Energy Research Institute's Health Physics and Dosimetry Services Group and Radioactivity Measurement Group.

Compliance with ethical standards

Conflicts of interest The author declares that he has no financial or non-financial interests in the subject matter or materials addressed in this article.

References

1. IAEA (2003) Extent of environmental contamination by naturally occurring radioactive material (norm) and technological options for mitigation, Technical Report Series No.419. International Atomic Energy Agency, Vienna

2. IAEA (2006) Assessing the Need for Radiation Protection Measures in Work Involving Minerals and Raw Materials. Vienna

3. IAEA (2011) Exposure of the Public from Large Deposits of Mineral Residues. Vienna

4. IAEA (2013) Management of NORM Residues, IAEA-TECDOC-1712, International Atomic Energy Agency. Vienna

5. Skipperud L, Strømman G, Yunusov M, et al (2013) Environmental impact assessment of radionuclide and metal contamination at the former U sites Taboshar and Digmai, Tajikistan. J Environ Radioact 123:50–62. https://doi.org/10.1016/j.jenvrad.2012.05.007

6. Borai EH, el Afifi EM, Shahr El-Din AM (2017) Selective elimination of natural radionuclides during the processing of high grade monazite concentrates by caustic conversion method. Korean Journal of Chemical Engineering 34:1091–1099. https://doi.org/10.1007/s11814-016-0350-9

7. Jirásek J, Matýsek D, Alexa P, et al (2020) High Specific Activity of Radium Isotopes in Baryte from the Czech Part of the Upper Silesian Basin—An Example of Spontaneous Mine Water Treatment. Minerals 10:103. https://doi.org/10.3390/min10020103

8. Chałupnik S, Franus W, Wysocka M, Gzyl G (2013) Application of zeolites for radium removal from mine water. Environmental Science and Pollution Research 20:7900–7906. https://doi.org/10.1007/s11356-013-1877-5

9. Alnour IA, Wagiran H, Ibrahim N, et al (2014) Gross alpha and gross beta activity in the products and by-product of amang tin tailings process. J Radioanal Nucl Chem. https://doi.org/10.1007/s10967-014-3708-7

10. Carvalho FP, Tufa MB, Oliveira JM, Malta M (2021) Radionuclides and Radiation Exposure in Tantalite Mining, Ethiopia. Arch Environ Contam Toxicol 81:648–659. https://doi.org/10.1007/s00244-021-00858-8

11. El-Afifi EM, Shahr El-Din AM, Aglan RF, et al (2017) Baseline evaluation for natural radioactivity level and radiological hazardous parameters associated with processing of high grade monazite. Regulatory Toxicology and Pharmacology 89:215–223. https://doi.org/10.1016/j.yrtph.2017.07.029

12. Arogunjo AM, Höllriegl V, Giussani A, et al (2009) Uranium and thorium in soils, mineral sands, water and food samples in a tin mining area in Nigeria with elevated activity. J Environ Radioact 100:232–240. https://doi.org/10.1016/j.jenvrad.2008.12.004

13. Leopold K, Michalik B, Wiegand J (2007) Availability of radium isotopes and heavy metals from scales and tailings of Polish hard coal mining. J Environ Radioact 94:137–150. https://doi.org/10.1016/j.jenvrad.2007.01.002

14. MTA (2022) Copper. In: Mineral Research and Exploration General Directorate. https://www.mta.gov.tr/v3.0/metalik-madenler/bakir. Accessed 14 Jan 2022

15. BMLRT (2021) Production of Mineral Raw Materials of individual Countries by Minerals. In: World Mining Data, Austrian Federal Ministry of Agriculture, Regions and Tourism . https://www.world-mining-data.info/?World_Mining_Data___Data_Section. Accessed 20 Jan 2022

16. Kırıs E, Baltas H (2021) Assessing pollution levels and health effects of heavy metals in sediments around Cayeli copper mine area, Rize, Turkey. Environ Forensics 22:372–384. https://doi.org/10.1080/15275922.2020.1850572

17. Kasowska D, Gediga K, Spiak Z (2018) Heavy metal and nutrient uptake in plants colonizing post-flotation copper tailings. Environmental Science and Pollution Research 25:824–835. https://doi.org/10.1007/s11356-017-0451-y

18. Rzymski P, Klimaszyk P, Marszelewski W, et al (2017) The chemistry and toxicity of discharge waters from copper mine tailing impoundment in the valley of the Apuseni Mountains in Romania. Environmental Science and Pollution Research 24:21445–21458. https://doi.org/10.1007/s11356-017-9782-y

19. EPA (1999) Technologically Enhanced Naturally Occurring Radioactive Materials in the Southwestern Copper Belt of Arizona, Technical Report EPA 402-R-99-002, U.S. Environmental Protection Agency. Washington DC

20. Nguyen DC, Khanh P le, Jodłowski P, et al (2016) Natural Radioactivity at the Sin Quyen Iron-Oxide-Copper-Gold Deposit in North Vietnam. Acta Geophysica 64:2305–2321. https://doi.org/10.1515/acgeo-2016-0103

21. Belyaeva O, Pyuskyulyan K, Movsisyan N, et al (2019) Natural radioactivity in urban soils of mining centers in Armenia: Dose rate and risk assessment. Chemosphere 225:859–870. https://doi.org/10.1016/j.chemosphere.2019.03.057

22. PÉREZ SÁNCHEZ D, PRENDES ALONSO M, CORCHO ALVARADO JA (2000) Exposure to natural radiation in gold–copper mines located in areas with high levels of natural radiation. In: Proc. 5th Int. Conf. on High Levels of Natural Radiation and Radon Areas: Radiation Dose and Health Effects (Abstract P1.3-239, p. 135). Munich

23. Benvenuti M, Mascaro I, Corsini F, et al (1997) Mine waste dumps and heavy metal pollution in abandoned mining district of Boccheggiano (Southern Tuscany, Italy). Environmental Geology 30:238–243. https://doi.org/10.1007/s002540050152

24. Salonen V-P, Tuovinen N, Valpola S (2006) History of Mine Drainage Impact on Lake Orijärvi Algal Communities, SW Finland. J Paleolimnol 35:289–303. https://doi.org/10.1007/s10933-005-0483-z

25. Brooks SJ, Udachin V, Williamson BJ (2005) Impact of copper smelting on lakes in the southern Ural Mountains, Russia, inferred from chironomids. J Paleolimnol 33:229–241. https://doi.org/10.1007/s10933-004-3936-x

26. Andrade S, Moffett J, Correa JA (2006) Distribution of dissolved species and suspended particulate copper in an intertidal ecosystem affected by copper mine tailings in Northern Chile. Mar Chem 101:203–212. https://doi.org/10.1016/j.marchem.2006.03.002

27. Ntengwe FW, Maseka KK (2006) The impact of effluents containing zinc and nickel metals on stream and river water bodies: The case of Chambishi and Mwambashi streams in Zambia. Physics and Chemistry of the Earth, Parts A/B/C 31:814–820. https://doi.org/10.1016/j.pce.2006.08.027

28. ZHOU J-M, DANG Z, CAI M-F, LIU C-Q (2007) Soil Heavy Metal Pollution Around the Dabaoshan Mine, Guangdong Province, China. Pedosphere 17:588–594. https://doi.org/10.1016/S1002-0160(07)60069-1

29. Sridharan M, Madhavi TCh (2021) Investigating the influence of copper slag on the mechanical behaviour of concrete. Mater Today Proc 46:3225–3232. https://doi.org/10.1016/j.matpr.2020.11.195

30. Zhang Y, Shen W, Wu M, et al (2020) Experimental study on the utilization of copper tailing as micronized sand to prepare high performance concrete. Constr Build Mater 244:118312. https://doi.org/10.1016/j.conbuildmat.2020.118312

31. Onuaguluchi O, Eren Ö (2016) Reusing copper tailings in concrete: corrosion performance and socioeconomic implications for the Lefke-Xeros area of Cyprus. J Clean Prod 112:420–429. https://doi.org/10.1016/j.jclepro.2015.09.036

32. Çayeli Bakır. https://www.cayelibakir.com/en/corporate.asp. Accessed 20 Jan 2022

33. Alkan N, Alkan A, Akbaş U, Fisher A (2015) Metal Pollution Assessment in Sediments of the Southeastern Black Sea Coast of Turkey. Soil and Sediment Contamination: An International Journal 24:290–305. https://doi.org/10.1080/15320383.2015.950723

34. Mani M, Altunışık A, Gedik K (2021) Bioaccumulation of Trace Elements and Health Risk Predictions in Edible Tissues of the Marsh Frog. Biol Trace Elem Res. https://doi.org/10.1007/s12011-021-03017-1

35. Yilmaz E (2000) Çayeli Bakır Cevherinin Flotasyonunda Kullanılan Kimyasal Reaktiflerin Zenginleştirmeye Etkisi (The Effect of Chemical Reagents Used for Flotation of Cayeli Copper Ore on the Recovery)

36. (2020) Nuclear Energy Research Institute-Turkish Energy, Nuclear and Mineral Research Agency. https://www.tenmak.gov.tr/en/#. Accessed 27 Jan 2022

37. Gilmore GR (2008) Practical Gamma-Ray Spectrometry, 2nd edition. John Wiley & Sons, Ltd, Chichester, UK

38. IAEA Reference Products for Environment and Trade. In: Sertified Reference Materials. https://nucleus.iaea.org/sites/ReferenceMaterials/Pages/RefmatArchive.aspx. Accessed 28 Jan 2022

39. AĞUŞ Y (2018) Gamma Spectrometric Method Validation for the Measurements of 40K and 137Cs in the Milk Powder. Süleyman Demirel University Journal of Natural and Applied Sciences 22:493–498. https://doi.org/10.19113/sdufbed.25850

40. Parmaksız A (2020) Radiological assessment of the bauxite mining in Turkey and estimation of radiation dose contribution of the red mud as a concrete agent of the model room by using RESRAD-BUILD computer code. J Radioanal Nucl Chem 326:1107–1118. https://doi.org/10.1007/s10967-020-07397-x

41. El-Taher A (2010) Gamma spectroscopic analysis and associated radiation hazards of building materials used in Egypt. Radiat Prot Dosimetry 138:166–173. https://doi.org/10.1093/rpd/ncp205

42. Currie LA (1968) Limits for qualitative detection and quantitative determination. Application to radiochemistry. Anal Chem 40:586–593. https://doi.org/10.1021/ac60259a007

43. RESA (2022) Radiation Early Warning System Network. https://www.ndk.org.tr/radyasyon-erken-uyari-sistemi-agi-resa. Accessed 2 Feb 2022

44. EURDEP (2022) European Radiological Data Exchange Platform. https://remap.jrc.ec.europa.eu/Simple.aspx. Accessed 2 Feb 2022

45. Bochiolo M, Verdoya M, Chiozzi P, Pasquale V (2012) Radiometric surveying for the assessment of radiation dose and radon specific exhalation in underground environment. J Appl Geophy 83:100–106. https://doi.org/10.1016/j.jappgeo.2012.05.004

46. Walencik-Łata A, Szkliniarz K, Kisiel J, et al (2022) Characteristics of Natural Background Radiation in the GIG Experimental Mine 'Barbara', Poland. Energies (Basel) 15:685. https://doi.org/10.3390/en15030685

47. Doyi I, Oppon OC, Glover ET, et al (2013) Assessment of occupational radiation exposure in underground artisanal gold mines in Tongo, Upper East Region of Ghana. J Environ Radioact 126:77–82. https://doi.org/10.1016/j.jenvrad.2013.07.007

48. Rana BK, Sahoo SK, Ravi PM, Tripathi RM (2014) Evaluation of occupational radiological exposures associated with a low ore grade underground uranium mine of Bagjata, India. J Radioanal Nucl Chem 301:9–16. https://doi.org/10.1007/s10967-014-3123-0

49. Mokobia CE (2004) Background gamma terrestrial dose rate in Nigerian functional coal mines. Radiat Prot Dosimetry 108:169–173. https://doi.org/10.1093/rpd/nch003

50. Tresnjo Z, Adrovic J, Hankic E (2017) Levels of Radon Activity Concentration and Gamma Dose Rate in Air of Coal Mines in Bosnia and Herzegovina. In: Radon. InTech

51. IAEA (2014) Radiation Protection and Safety of Radiation Sources: International Basic Safety Standards-IAEA Safety Standards-General Safety Requirements Part 3. Vienna

52. United Nations Scientific Committee on the Effects of Atomic Radiation (2010) Sources and Effects of Ionizing Radiation-UNSCEAR 2008 Report-Volume I: SOURCES Report to the General Assembly Scientific Annexes A and B

53. IAEA (2004) Application of the Concepts of Exclusion, Exemption and Clearance. Safety Standard Series No. RS-G-1.7. IAEA.

54. Krieger R (1981) Radioactivity of Construction Materials. Betonwerk Fertigteil Technik 47:468–473

55. Beretka J, Mathew PJ (1985) Natural Radioactivity of Australian Building Materials, Industrial Wastes and By-products. Health Phys 48:87–95. https://doi.org/10.1097/00004032-198501000-00007

56. European Commission (EC) (1999) Radiological Protection Principles concerning the Natural Radioactivity of Building Materials, Radiation Protection 112 Official Publications of the European Communities. Luxembourg

57. Turhan Ş, Kurnaz A, Karataşlı M (2022) Evaluation of natural radioactivity levels and potential radiological hazards of common building materials utilized in Mediterranean region, Turkey. Environmental Science and Pollution Research 29:10575–10584. https://doi.org/10.1007/s11356-021-16505-7

58. UNSCEAR (2000) Sources and effects of ionizing Radiation, United Nations Scientific Committee on the Effects of Atomic Radiation UNSCEAR 2000 Report to the General Assembly, with Scientific Annexes. New York-USA

59. IAEA Safety Standards for protecting people and the environment GSGNoG-8 (2018) Radiation Protection of the Public and the Environment. Vienna

60. Qureshi AA, Tariq S, Din KU, et al (2014) Evaluation of excessive lifetime cancer risk due to natural radioactivity in the rivers sediments of Northern Pakistan. J Radiat Res Appl Sci 7:438–447. https://doi.org/10.1016/j.jrras.2014.07.008

61. ICRP (1991) 1990 Recommendations of the International Commission on Radiological Protection. Vol. 21 No.1-3, publication 60

62. WHO (World Health Organization) (2022) The Global Health Observatory-Life expectancy. https://www.who.int/data/gho/data/indicators/indicator-details/GHO/life-expectancy-at-birth-(years). Accessed 16 Feb 2022

63. Esmaeili J, Aslani H, Onuaguluchi O (2020) Reuse Potentials of Copper Mine Tailings in Mortar and Concrete Composites. Journal of Materials in Civil Engineering 32:04020084. https://doi.org/10.1061/(ASCE)MT.1943-5533.0003145

64. Zhao F, Zhao J, Liu H (2009) Autoclaved brick from low-silicon tailings. Constr Build Mater 23:538–541. https://doi.org/10.1016/j.conbuildmat.2007.10.013

65. Huang X, Ni W, Cui W, et al (2012) Preparation of autoclaved aerated concrete using copper tailings and blast furnace slag. Constr Build Mater 27:1–5. https://doi.org/10.1016/j.conbuildmat.2011.08.034

66. Gupta RC, Mehra P, Thomas BS (2017) Utilization of Copper Tailing in Developing Sustainable and Durable Concrete. Journal of Materials in Civil Engineering 29:04016274. https://doi.org/10.1061/(ASCE)MT.1943-5533.0001813

67. Saxena M, Gowri VS (2002) Innovative building materials. Civil Engineering Construction Rev 15:64–50

68. Saxena M, Asokan P, Morchhale RK (2004) Durability characteristics of fired clay and clay fly ash bricks. In: Proceeding of the National Seminar on Recent Trends in Building Materials, RRL, Bhopal. pp 328–303

69. Sultan HA (1979) Stabilized copper mill tailings for highway construction Transp Res Rec, No. 734. In: 58th Annual Meeting of the Transportation Research Board. Washington District of Columbia, United States

70. Muleya F, Mulenga B, Zulu SL, et al (2021) Investigating the suitability and cost-benefit of copper tailings as partial replacement of sand in concrete in Zambia: an exploratory study. Journal of Engineering, Design and Technology 19:828–849. https://doi.org/10.1108/JEDT-05-2020-0186

71. Argonne National Laboratory RESRAD-BUILD. Residual radioactive in buildings. https://resrad.evs.anl.gov/codes/resrad-build/. Accessed 23 Feb 2022

72. Yu C, LePoire DJ, Cheng JJ, et al (2003) User's manual for RESRAD-BUILD Version 3. ANL/EAD/03-1

73. Abdullahi S, Ismail AF, Yasir MS (2020) Radiological hazard analysis of Malaysia's ceramic materials using generic and RESRAD-BUILD computer code approach. J Radioanal Nucl Chem 324:301–315. https://doi.org/10.1007/s10967-020-07070-3

74. Pepin S (2018) Using RESRAD-BUILD to assess the external dose from the natural radioactivity of building materials. Constr Build Mater 168:1003–1007. https://doi.org/10.1016/j.conbuildmat.2018.02.015

75. Ismail AF, Abdullahi S, Samat S, Yasir MS (2018) Radiological Dose Assessment of Natural Radioactivity in Malaysian Tiles using Resrad-Build Computer Code. Sains Malays 47:1017–1023. https://doi.org/10.17576/jsm-2018-4705-18

76. EU (2013) Council Directive 2013/59 Euratom of 5 December 2013 laying down basic safety standards for protection against dangers arising from exposure to ionising radiation, and repealing directives 89/618/Euratom, 90/641/Euratom, 96/29/Euratom, 97/43/Euratom and 2